Cattaneo-Christov Heat Flux Model in the Flow of Non-Newtonian Liquid

By

Muhammad Waleed Ahmed Khan

CERTIFICATE

A DISSERTATION SUBMITTED IN THE PARTIAL FULFILLMENT OF THE REQUIREMENTS FOR THE DEGREE OF THE MASTER OF PHILOSOPHY

We accept this dissertation as conforming to the required standard

1. ______________________
Prof. Dr. Muhammad Ayub
(Supervisor)

2. ______________________
Prof. Dr. Muhammad Ayub
(Chairman)

3. ______________________
Prof. Dr. Akhtar Hussain
(External Examiner)

Department of Mathematics
Quaid-I-Azam University
Islamabad, Pakistan

2016

Preface

Heat transfer existing due to the temperature difference between two bodies or within the bodies at different temperatures has important role in our daily life. Thus the researchers and scientists have focused on heat transfer phenomenon via Fourier's law [1] of heat conduction. This law provides a basis for the study of heat transfer phenomenon. Fourier's law of heat conduction via parabolic equation provides sufficient information in the sense that any initial interruption is felt immediately throughout the whole substance. To overcome this issue Cattaneo [2] added a thermal relaxation time which allows the transfer of heat through propagation of heat waves with finite speed. This expression was later modified by Christov [3], by taking thermal relaxation time along with Oldroyd's upper-convected derivatives. Cattaneo-Christov model in thermal convection flow was analyzed by Straughan [4]. The uniqueness of this model for the flow of incompressible fluids was observed by Tibulle and Zampoli [5]. The same model in the boundary layer stretched flow of Maxwell fluid was presented by Han et al.[6]. Characteristics of Cattaneo-Christov heat flux model in rotating flow of Maxwell fluid over a linear stretching sheet were studied by Mustafa [7]. Hayat et al. [8] studied the Cattaneo-Christov heat flux model in the flow of Maxwell fluid induced by a stretching sheet with variable thickness.

The use of boundary layer stretched flow with heat transfer has drawn the attention of researchers and scientists due to their vast applications in many areas of industrial manufacturing, metallurgical and engineering processes. Motion of a surface in cooling medium is a tool for the process of heat treatment. In order to avoid the metals from molten state, metals are heated and cooled in a regular pattern during this process. The purpose of heat treating process is to enhance properties of metals e.g strength, hardness and resistivity etc. Metals are also made softer and pliable by heating processes. Few applications here consist of glass blowing, polymer extrusion, crystal growth, drawing plastic films, paper production, annealing of metals, manufacturing artificial fibers, extrusion of sheets, aerodynamics etc. The raw material in many industrial processes is passed through the die for the extrusion in liquefied form under high temperature. Zheng et al. [9] studied the unsteady boundary layer flow over a permeable stretching sheet with non-uniform heat generation/absorption. MHD flow of a nanofluid over stretching sheet was studied by Rashidi et al. [10]. The behavior of MHD mixed convection in flow over a permeable inclined stretching surface with Ohmic heating and thermal radiation was studied by Su et al. [11]. Three-dimensional MHD flow of viscoelastic fluid over a stretching sheet was studied by Turkyilmazoglu [12]. Zheng et al. [13] discussed velocity slip and temperature jump of MHD flow over a shrinking surface. Boundary layer stagnation point flow of Jeffrey fluid towards a stretching sheet was discussed by Hayat et al. [14] taking convective boundary conditions. Unsteady radiative mixed convection flow of Maxwell fluid past a permeable sheet with slip velocity and non-uniform heat generation/absorption effects was analyzed by Zheng et al. [15]. Mukhopadhyay et al. [16] studied thermo-solutal stratification effect in the boundary layer flow of viscous fluid over a permeable stretching sheet. Stagnation point flow of an Oldroyd-B fluid in a thermally stratified medium was discussed by Hayat et al. [17]. Properties of nanofluid in a rotating system with stretching sheet were analyzed by Sheikholeslami and Ganji [18]. It is noted that boundary layer flow over stretching surface through different aspects has been studied extensively. In such studies the surface is not considered of variable thickness. No doubt such consideration is important in civil, mechanical, marine and aeronautical designs. Variable sheet thickness is used for the reduction of structural element weight. It also improves the utility of the material more frequently in various industrial processes. Very few attempts for flow over variable thicked surface have been made. For example flow of viscous fluid over a sheet with variable thickness was analyzed by Fang et al. [19]. Khader and Megahed [20] studied slip velocity effects in the boundary layer flow over a nonlinear stretching sheet with variable thickness. Heat transfer properties in the flow of nanofluid over a nonlinear stretching sheet with variable thickness are studied by Wahed et al. [21].

This dissertation consists of three chapters. First chapter contains some basic concepts, definitions and equations related to the next two chapters. Second chapter presents slip effect on the flow due to non-linear stretching surface of variable thickness. Appropriate transformations reduce the partial differential system into ordinary differential system. Homotopy analysis technique is used to solve the governing nonlinear differential equations. The effects of various physical parameters on velocity profile are shown graphically. Third chapter is the extension work which presents Cattaneo-Christov heat flux effect over a stretching sheet having variable thickness along with heat generation and variable thermal conductivity. Cattaneo-Christov heat flux model is used rather than classical Fourier's of heat conduction in present flow analysis.

Resulting partial differential system of equations is transformed to ordinary differential system by using suitable transformations. Convergent series solutions are computed through homotopy analysis technique [22-29]. Behaviors of various parameters on velocity and temperature profiles are sketched and discussed.

Contents

Chapter 1

Basic definitions and equations

1.1 Introduction

This chapter has been arranged through some definitions and equations which are useful for the next two chapters.

1.2 Some concepts about fluid

1.2.1 Fluid

A substance deforming continuously under the action of applied shear stress is called fluid.

1.2.2 Fluid mechanics

The branch of engineering dealing with the fluids either at rest or in motion. Some common engineering fluids are air (a gas), steam (a vapor) and water (a liquid).

Fluid mechanics can be divided into two categories:

1. The study of fluids at rest is called statics.

2. The study of fluids in motion is called dynamics.

1.2.3 Types of flow system

Internal flow system

Fluid flows surrounded by closed boundaries or surfaces are termed as internal flow systems. Examples are flow through pipes, valves, ducts, or open channels.

External flow system

Flows having no specific boundaries are termed as external flows. Flow around aeroplane wings, automobiles, buildings or ocean water through which ships, submarines and torpedoes move/sail.

Internal and external flow systems may be laminar, turbulent, compressible or incompressible.

1.2.4 Body force

A force acting throughout the volume of a body without any physical contact. Examples are gravity and electromagnetic forces.

1.2.5 Inertial forces

A force which resists a change in state of an object.

1.2.6 Surface force

A force that acts across an internal or external element in a body through direct physical contact. Pressure and shear forces are examples of surface force.

1.2.7 Shear stress

It is the component of the stress coplanar with the cross section area of a material. The internal forces that neighboring particles of a continuous material exert on each other is called shear stress. It is denoted by a Greek letter τ.

1.2.8 Normal stress

The component of the stress normal to cross section of a material is called normal stress. It is denoted by σ.

1.2.9 Viscosity

Viscosity of fluid is the measure of its internal resistance to deformation caused by tensile or shear stress. A fluid having no resistance to shear stress is called ideal or inviscid liquid. Super fluids have zero viscosity. Viscosity depends on composition and temperature of a fluid. It is also called dynamic/absolute viscosity. It is denoted by μ and is given by

$$\mu = \frac{shear\ stress}{shear\ strain}.$$

Viscosity is measured in $kg/m.sec$ and is having dimensions of

$$[\frac{M}{LT}].$$

1.2.10 Kinematic viscosity

The ratio of absolute viscosity to density of fluid is called kinematic viscosity. It is given by

$$\nu = \frac{\mu}{\rho}.$$

It is measured in $m^2/\sec$. It is having dimensions of

$$[\frac{L^2}{T}].$$

1.2.11 Flow types

1) Laminar flow

The flow pattern in which fluid flows in parallel smooth layers with no crossing over between the layers. Smoke rising from a cigarette to the first few centimeters in a still surrounding shows a clear picture of laminar flow.

2) Turbulent flow

Turbulent flow is a less orderly flow regime, characterizes the pattern of the flow in which the fluid particles have no specific paths or trajectories. Break up of rising smoke into random and haphazard motion represents turbulent flow.

1.2.12 Newton's law of viscosity

It states that

$$\begin{aligned} \tau_{yx} &\propto \frac{du}{dy}, \\ \tau_{yx} &= \mu\frac{du}{dy}, \end{aligned}$$

in which μ is the absolute viscosity.

1.2.13 Newtonian fluids

Those fluids which obey Newton's law of viscosity are termed as Newtonian fluids. Water, air and gases are Newtonian fluids.

1.2.14 Non-Newtonian fluids

Those fluids which do not obey Newton's law of viscosity are termed as non-Newtonian or we can say that those fluid for which shear stress is non-linearly proportional to shear strain. Since viscosity depends upon nature of the fluids so for such fluids viscosity remains no more constant and it becomes a function of applied shear stress. Examples of such fluids consist of honey, toothpaste, ketchup, paint etc. Mathematically

$$\begin{aligned} \tau_{yx} &\propto \left(\frac{du}{dy}\right)^n, n \neq 1 \\ \tau_{yx} &= \eta\left(\frac{du}{dy}\right), \\ \eta &= \kappa\left(\frac{du}{dy}\right)^{n-1}. \end{aligned}$$

Here η represents the apparent viscosity, n flow behavior index and κ consistency index. It reduces to Newton's law of viscosity when $n = 1$. Depending upon n (flow behavior index) and apparent viscosity, non-Newtonian fluids are further divided into many subclasses.

Non-Newtonian fluids are mainly classified into three types:

1. Rate type fluids.

2. Integral type fluids.

3. Differential type fluids.

We will discuss only rate type fluids here.

1.2.15 Rate type materials

Such materials predict the relaxation and retardation times effects. Maxwell, Oldroyd and Burger fluids belong to this class.

Relaxation time

The time required for coming back of a perturbed system into its equilibrium state.

Retardation time

The time required for the process of balancing the applied shear stress by the opposing forces produced during deformation.

1.3 Mechanisms of heat transfer

Heat transfer occurs from region of higher kinetic energy towards the region of lower kinetic energy or simply from hotter to colder regions. Temperature difference in between the two regions is the main reason for heat to flow. Heat transfers from one place to another by different processes, depending upon the nature of material under consideration.

1.3.1 Conduction

Particles are in constant motion. During motion of the particles, collisions occur, which result in the exchange of kinetic energies. So the process of heat transfer from one place to another due to collision of molecules/particles is called conduction. Such type of heat transfer is observed in solids e.g heated rod at one end, here no material flow occurs physically.

1.3.2 Convection

It is the process of heat transfer during which particles having more kinetic energies replace the particles with less kinetic energies. The transfer of heat occurs due to random Brownian motion of individual particles from hotter to colder region, and this process is known as convection.

1.3.3 Types of convection

Natural convection

The transfer of heat that occurs only due to temperature difference is called natural convection. Dense particles of fluid fall, while lighter particles rise, resulting the bulk motion of fluids. Natural convection can only occurs in the presence of gravitational force.

Forced convection

To increase the rate of heat exchange, fluid motion is generated by external surface forces such as fan, pump etc. Force convection is more efficient than natural convection.

Mixed convection

The process in which heat transfer occurs due to both natural and forced convection is termed as mixed convection.

1.3.4 Radiation

The transmission of heat energy in the form of electromagnetic waves with or without any medium is termed as radiation. Examples are fire, sunlight and very hot objects etc.

1.4 Some concepts about heat

1.4.1 Heat source/sink

Any object which produces and emits heat is termed as a heat source and any object that dissipates heat is termed as a heat sink. Nuclear reactors, sun, fire and electric heaters are heat sources while semiconductors, light emitting diodes, fans and solar cells are examples of heat sink.

1.4.2 Thermal conductivity

Therm means heat and conduction is transfer by collision of molecules. So it is measure of the ability of material to transmit heat from one place to another. Or it can also be defined as the amount of heat transfer through a unit thickness of a substance, in a direction perpendicular to surface area due to unit temperature gradient. It is denoted by k and is given by

$$k = \frac{Ql}{A\Delta T},$$

where Q denotes heat flow in a unit time, A is area of cross section and ΔT denotes change in temperature. In SI system thermal conductivity is measured in $W/m.K$, having dimensions of

$$[\frac{ML}{T^3\theta}].$$

1.4.3 Thermal diffusivity

It is measure of ability of a substance to transfer heat energy relative to its ability to store heat energy. Thermal diffusivity is measured in $m^2/\sec$, denoted by α and is given by

$$\alpha = \frac{k}{\rho c_p},$$

where k is thermal conductivity, c_p is specific heat and ρ is density.

Thermal diffusivity measures the property of a material for unsteady heat conduction. This describes how quickly a material responds to change in temperature.

1.4.4 Specific heat

It is an extensive property of a material defined as the amount of heat energy required to increase temperature of the material by 1^0C. It is measured in $\frac{J}{K}$, having the dimensions of

$$[\frac{L^2M}{T^2\theta}].$$

1.4.5 Newton's law of heating

The rate of heat loss of a body is directly proportional to temperature difference between the body and its surrounding.

1.4.6 Fourier's law of heat conduction

It is defined as the rate of heat conduction through a homogeneous material is directly proportional to negative gradient of temperature. Mathematically

$$\begin{aligned} q &\propto -\Delta T, \\ q &= -k\Delta T, \end{aligned}$$

q is heat flux density, which is the amount of energy flow through a unit area per unit time. q is measured in $\frac{W}{m^2}$, k is material's thermal conductivity and ΔT is temperature gradient.

1.4.7 Cattaneo-Christov heat flux

In the present dissertation Cattaneo-Christov heat flux is used rather than classical Fourier's law of heat conduction. In order to overcome the deficiency that arose in classical Fourier's law, Cattaneo added a thermal relaxation time to the system. After that, Christov modified the same model by taking a thermal retardation time.

1.4.8 Oldroyd-B fluid

Many complex fluids are having viscous and elastic effects under shear stress. Polymer solutions, toothpaste, oil and clay are some examples.

One of the simplest constitute model that describes viscoelastic behavior of polymer solutions is the Oldroyd-B fluid model. This model is actually the extension of upper convected Maxwell model. The stress tensor for an Oldroyd-B fluid model is represented by

$$\mathbf{S} + \lambda_1 \frac{d\mathbf{S}}{dt} = \mu \left(1 + \lambda_2 \frac{D}{Dt}\right) \mathbf{A}_1,$$

where λ_1 and λ_2 are relaxation and retardation times respectively. This model gives good approximation of viscoelastic fluids flow. However, it is not able to predict shear thinning and shear thickening effects.

1.5 Dimensionless parameters

1.5.1 Prandtl number

Conduction and convection occur in fluids. For the process of heat transfer, temperature difference is the main cause. Rate of conduction and convection vary in different fluids.

Prandtl number is used to determine the domination of either conduction or convection. It is defined as the ratio of momentum to thermal diffusion rate. It is denoted by Pr and given by

$$\mathrm{Pr} = \frac{\nu}{\alpha},$$

where ν is kinematic viscosity and α is thermal diffusion rate. For many gases over a vast range of temperature and pressure, Pr is approximately treated as constant.

1.5.2 Reynolds number

A dimensionless parameter used to predict flow pattern for different fluid flow situations. It measures the ratio of inertial to viscous forces and relative importance of the two forces for given flow conditions. It is denoted by Re named after Osborne Reynolds, and is given as

$$\begin{aligned} \mathrm{Re} &= \frac{inertial\ force}{viscous\ force}, \\ \mathrm{Re} &= \frac{\rho V L}{\mu} = \frac{VL}{\nu}, \end{aligned}$$

V is max velocity, L is length of geometry.

For low Reynolds number, viscous forces are more dominant than inertial forces, laminar flow occurs which characterizes a constant and smooth fluid motion. Similarly, for higher Reynolds number, inertial forces are more dominant than viscous forces, hence turbulent flow occurs.

1.5.3 Nusselt number

It is defined as a quantity that measures ratio of convective to conductive heat transfer coefficients. It has the involvement of Newton's law of cooling/heating and Fourier's law of heat conduction. It is denoted by Nu named after Wihlem Nusselt.

1.5.4 Deborah number

A dimensionless parameter used to specify fluidity of materials. It is defined as ratio of relaxation time to observation time. This specifies both elastic and viscous properties of materials. The higher the Deborah number, the closer it is to a perfect solid.

Mathematically

$$De = \frac{t_c}{t_p},$$

here t_c is stress relaxation time and t_p is observation time scale.

1.5.5 Eckert number

A dimensionless parameter used to determine the relative importance of kinetic energy in a heat transfer phenomenon. It shows the relationship between kinetic energy and boundary layer enthalpy difference. It is denoted by Ec and given by

$$Ec = \frac{u^2}{c_p \Delta T},$$

where u is fluid velocity, c_p is specific heat and ΔT is temperature difference. Ec is used to characterize heat dissipation.

1.5.6 Hartman number

A dimensionless parameter used to determine relative importance of drag force resulting from magnetic and viscous forces.

It is defined as the ratio of magnetic to viscous forces given by

$$M = \frac{magnetic\ forces}{viscous\ forces} = B_0 d\sqrt{\frac{\sigma}{\mu}},$$

where B_0 shows characteristic value of magnetic induction, d is characteristic length and μ is dynamic viscosity coefficient.

1.6 Flow equations

1.6.1 Continuity equation

Consider flow of mass m through a control volume V, we have

Rate of accumulation of mass in V + net mass flux = 0

or

$$\frac{\partial}{\partial t}\int\limits_v \rho dV + \int\limits_A \rho u.ndA = 0,$$

or

$$\int\limits_v \frac{\partial}{\partial t}\rho dV + \int\limits_A \rho U.ndA = 0,$$

by divergence theorem we have

$$\int\limits_v \left(\frac{\partial \rho}{\partial t} + \nabla.\rho u\right) dV = 0,$$

or

$$\frac{\partial \rho}{\partial t} + \nabla.\rho U = 0$$

This expression of mass conservation is known as equation of continuity. If material is incompressible we have

$$\nabla.U = 0.$$

The velocity field of an incompressible fluid is solenoidal. In rectangular coordinates system, having velocity components u, v and w, equation of continuity is given as

$$\frac{\partial u}{\partial x}+\frac{\partial v}{\partial y}+\frac{\partial w}{\partial z}=0.$$

Similarly, in electromagnetism, equation of continuity expresses charge conservation.

Mathematically

$$\nabla . j=-\frac{\partial \rho}{\partial t},$$

where j is current density and ρ is charge density.

Equation of continuity is also used in heat and energy, probability distribution, special and general relativity, quantum mechanics and particle physics etc.

1.6.2 Equation of motion

Equation of motion for fluids has been derived from law of conservation of linear momentum which shows that in the absence of external forces the total linear momentum for a system remains conserved. This law has been deduced from Newton's second law of motion.

Mathematically equation of motion is given by

$$\rho \frac{d\mathbf{V}}{dt}=\operatorname{div}\mathbf{T}+\rho\mathbf{b},$$

$\mathbf{T}$ is Cauchy stress tensor.

Left hand side shows inertial forces, first term on right hand side shows surface forces (external forces) and last term is internal (body) force.

Cauchy stress tensor is defined as

$$\mathbf{T}=-PI+\mathbf{S},$$

where S is extra stress tensor, depending upon nature of the fluid e.g

For Newtonian fluid

$$\mathbf{S}=\mu\mathbf{A}_1,$$

and for second grade fluid

$$\mathbf{S} = \mu \mathbf{A}_1 + \alpha_1 \mathbf{A}_2 + \alpha_2 \mathbf{A}_1^2,$$

here $\mathbf{A}_1$ and $\mathbf{A}_2$ are first and second Rivelin Erickson tensors respectively.

1.6.3 Energy equation

According to energy conservation law

$$\rho c_p \frac{dT}{dt} = -\operatorname{div} q,$$

and

$$\operatorname{div} q = -k \boldsymbol{\nabla} T.$$

Here ρ is fluid density, c_p is specific heat, T is temperature, κ is thermal conductivity. In above equation first term on left hand side shows total rate of change of energy, which is further divided into local and convective rate of change of energies. Right hand side comes from Fourier's law of heat conduction.

1.7 Solution method

1.7.1 Homotopic technique

HAM technique is one of the best and simplest technique for obtaining convergent series solution for weakly as well as strongly non-linear equations. This method uses the concept of homotopy from topology. Two functions are homotopic if one function continuously deforms into other function, e.g. $f_1(x)$ and $f_2(x)$ are two functions and F^* is a continuous mapping, then

$$F^* : X \times [0,1] \rightarrow Y$$

such that

$$F^*(x, 0) = f_1(x)$$

and

$$F^{*}(x,1)=f_2(x)$$

Lio in 1992 used the homotopic technique for obtaining convergent series solution.

HAM distinguishes itself from other techniques in the following ways:

1. It is independent of small/large parameter.
2. Convergent solution is guaranteed.
3. Freedom for the choice of base functions and linear operators.

Consider a non-linear differential equation

$$\mathcal{N}[u(x)]=0,$$

where $\mathcal{N}$ represents non-linear operator, and $u(x)$ is the unknown function.

Using parameter $p\in[0,1]$, a system of equations is constructed.

$$(1-p)\,\mathcal{L}\left[\widehat{u}\,(x;p)-u_0\,(x;p)\right]=p\hbar\mathcal{N}\widehat{u}\,(x;p)\,,$$

where $\mathcal{L}$ is linear operator, p is embedding parameter and $\hbar$ is convergence parameter. By putting value of p from 0 to 1, unknown function gets the value from $u_0(x)$ to $u(x)$.

Chapter 2

Slip effect on flow due to non-linear stretching surface of variable thickness

2.1 Introduction

This chapter reports the development of homotopy solution for flow of viscous fluid. Fluid is bounded by a non-linear stretching surface with variable thickness. In addition velocity slip condition is imposed. Appropriate transformations reduce the partial differential systems into the ordinary differential systems. The resulting systems are solved by homotopy technique. The results for velocity and temperature are established and discussed

Geometry of the given problem is

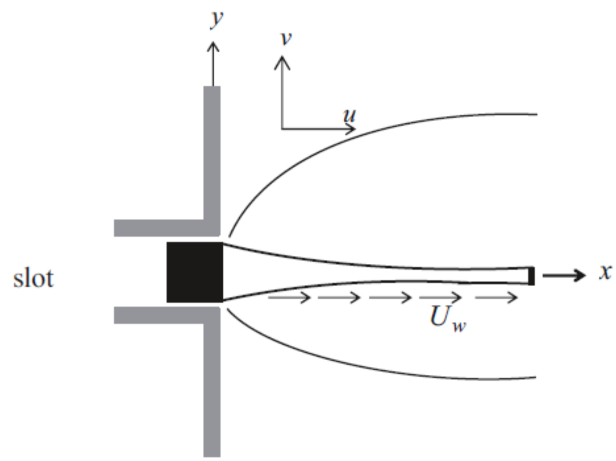

Fig.1 Schematic diagram of the problem

2.2 Mathematical formulation

Consider flow of an incompressible two dimensional viscous fluid over an impermeable stretching sheet. Slit is considered to be the origin of geometry. Sheet is stretched with a velocity $U_w = U_0 (x + b)^n$. Thickness of the sheet is taken variable, i.e. $y = A (x + b)^{\frac{1-n}{2}}$, where n is velocity power index and A is constant. The problem is considered for $n \neq 1$.

Governing equations for flow are

$$\nabla.\mathbf{V} = \mathbf{0}, \tag{2.1}$$

and

$$\rho \frac{d\mathbf{V}}{d\bar{t}} = \operatorname{div} \mathbf{T} + \boldsymbol{\rho}\mathbf{B}. \tag{2.2}$$

In absence of body forces we have

$$\rho \frac{d\mathbf{V}}{d\bar{t}} = \operatorname{div} \mathbf{T}, \tag{2.3}$$

where $\mathbf{T}$ is Cauchy stress tensor given by

$$\mathbf{T} = -P\mathbf{I} + \mu \mathbf{A}_1, \tag{2.4}$$

where μ is dynamic viscosity and A_1 is first Rivelin Erickson tensor.

For velocity

$$\mathbf{V} = (u(x,y), v(x,y), 0)\,, \tag{2.5}$$

$$\mathbf{A}_1 = \operatorname{grad}\mathbf{V} + (\operatorname{grad}\mathbf{V})^T\,, \tag{2.6}$$

Now Eq. (2.1) and (2.2) yield

$$\frac{\partial u}{\partial x} + \frac{\partial v}{\partial y} = 0, \tag{2.7}$$

$$\rho\left(\frac{\partial}{\partial t} + u\frac{\partial}{\partial x} + v\frac{\partial}{\partial y}\right)u = \frac{\partial \mathbf{T}_{xx}}{\partial x} + \frac{\partial \mathbf{T}_{xy}}{\partial y}, \tag{2.8}$$

$$\rho\left(\frac{\partial}{\partial t} + u\frac{\partial}{\partial x} + v\frac{\partial}{\partial y}\right)v = \frac{\partial \mathbf{T}_{yx}}{\partial x} + \frac{\partial \mathbf{T}_{yy}}{\partial y}, \tag{2.9}$$

In absence of pressure gradient and taking steady flow, we get the following form

$$\rho\left(u\frac{\partial}{\partial x} + v\frac{\partial}{\partial y}\right)u = \frac{\partial \mathbf{T}_{xx}}{\partial x} + \frac{\partial \mathbf{T}_{xy}}{\partial xy}, \tag{2.10}$$

$$\rho\left(u\frac{\partial}{\partial x} + v\frac{\partial}{\partial y}\right)v = \frac{\partial \mathbf{T}_{yx}}{\partial x} + \frac{\partial \mathbf{T}_{yy}}{\partial y}. \tag{2.11}$$

By taking boundary layer approximations one has

$$\frac{\partial u}{\partial x} + \frac{\partial v}{\partial y} = 0, \tag{2.12}$$

$$\left(u\frac{\partial}{\partial x} + v\frac{\partial}{\partial y}\right)u = \nu\frac{\partial^2 u}{\partial y^2}. \tag{2.13}$$

Here ν is kinematic viscosity and u and v are velocity components along x and y directions respectively. The associated boundary conditions are as follows

$$u\left(x, A(x+b)^{\frac{1-n}{2}}\right) = U_w + \lambda_1\frac{\partial u}{\partial x}, \quad v\left(x, A(x+b)^{\frac{1-n}{2}}\right) = 0, \tag{2.14}$$

$$u(x,\infty) = 0, \tag{2.15}$$

where λ_1 represents the slip coefficient and is given by

$$\lambda_1 = (x+b)^{\frac{1-n}{2}}. \tag{2.16}$$

Using the following transformations

$$\eta=\sqrt{\frac{(n+1)U_0\left(x+b\right)^{n-1}}{2\nu}}y, \qquad \psi(x,y)=\sqrt{\frac{2\nu U_0\left(x+b\right)^{n+1}}{n+1}}F\left(\eta\right), \tag{2.17}$$

and expressing u and v in terms of stream function $\psi(x,y)$ we have:

$$u=\frac{\partial\psi}{\partial y}, \quad v=-\frac{\partial\psi}{\partial x}. \tag{2.18}$$

We adopt

$$u=U_0(x+b)F'\left(\eta\right), \; v=-\sqrt{\frac{(n+1)\nu U_0\left(x+b\right)^{n-1}}{2}}\left(F(\eta)+\eta\frac{n-1}{n+1}F'(\eta)\right). \tag{2.19}$$

Using the above equations, conservation law of mass is satisfied and the resulting equations are as follows

$$F'''+FF''-\frac{2n}{n+1}F'^2=0, \tag{2.20}$$

with associated boundary conditions by

$$F\left(\alpha\right) = \frac{\alpha(1-n)}{1+n}F'(\alpha), \tag{2.21}$$

$$F'(\alpha) = 1+\lambda F''(\alpha), \quad F'\left(\infty\right)\rightarrow 0. \tag{2.22}$$

Here λ is slip velocity coefficient and α is the wall thickness parameter given by

$$\alpha=\sqrt{\frac{U_0(n+1)}{2\nu}}, \tag{2.23}$$

and η shows the plate surface.

For converting the domain from $[\alpha,\infty)$ to $[0,\infty)$, we use another transformation

$$F(\xi)=F(\eta-\alpha)=f(\eta). \tag{2.24}$$

Resulting equation is

$$f'''+ff''-\frac{2n}{n+1}f'^2=0, \tag{2.25}$$

and boundary conditions are

$$f(0) = \frac{\alpha(1-n)}{1+n} f'(0), \tag{2.26}$$

$$f'(0) = 1 + \lambda f''(0), \quad f'(\infty) \to 0, \tag{2.27}$$

Skin friction coefficient is a physical quantity of primary importance which is given by

$$C_{fx} = -2\sqrt{\frac{m+1}{2}} R_{ex}^{-\frac{1}{2}} f''(0). \tag{2.28}$$

2.3 Solution methodology

Using homotopy analysis method, initial guess and linear operator must be taken so that initial guess must satisfy the boundary conditions. Initial guess and linear operator taken here are

$$f_0(\eta) = \frac{1}{1+\lambda}\left(\alpha\frac{1-n}{1+n} + 1 - \exp(-\eta)\right), \tag{2.29}$$

$$\mathcal{L}_f(f) = \frac{d^3 f}{d\eta^3} - \frac{df}{d\eta}, \tag{2.30}$$

satisfying the equation

$$\mathcal{L}_f\left[C_1 + C_2 \exp(\eta) + C_3 \exp(-\eta)\right] = 0, \tag{2.31}$$

where C_i,for $i = 1, 2, 3$ are arbitrary constants.

2.3.1 Zeroth order system

The corresponding zeroth order equations are

$$(1-p)\mathcal{L}_f\left[\widehat{f}(\eta;p) - f_0(\eta)\right] = p\hbar_f \mathcal{N}_f\left[\widehat{f}(\eta;p), \widehat{\theta}(\eta;p)\right], \tag{2.32}$$

$$\widehat{f}(0;p) = \alpha\frac{1-n}{1+n}(1 + \lambda\widehat{f}''(0;p)), \quad \widehat{f}'(\infty;p) \to 0, \tag{2.33}$$

$$\widehat{f}'(0;p) = 1 + \lambda\widehat{f}''(0;p), \tag{2.34}$$

where $\hbar_f$ represents non-zero auxiliary parameter, p is embedding parameter and $\mathcal{N}_f$ shows non-linear differential operator.

$$\mathcal{N}_f\left[\widehat{f}\left(\eta,p\right)\right]=\frac{\partial^3\widehat{f}\left(\eta;p\right)}{\partial\eta^3}+$$

$$+\widehat{f}\left(\eta;p\right)\frac{\partial^2\widehat{f}\left(\eta;p\right)}{\partial\eta^2}-\frac{2n}{n+1}\left(\frac{\partial\widehat{f}\left(\eta;p\right)}{\partial\eta}\right)^2. \tag{2.35}$$

By putting the values of p from 0 to 1, the function $f\left(\eta\right)$ takes the values from $f_0\left(\eta\right)$ to $f\left(\eta\right)$. By Taylor series expansion of $f\left(\eta\right)$ we have

$$\widehat{f}\left(\eta;p\right)=f_0\left(\eta\right)+\sum_{m=1}^{\infty}f_m\left(\eta\right)p^m,\qquad f_m\left(\eta\right)=\frac{1}{m!}\frac{\partial^m\widehat{f}\left(\eta;p\right)}{\partial p^m}\bigg|_{p=0}. \tag{2.36}$$

2.3.2 mth order approximation

The equations for mth order problem are

$$\mathcal{L}_f\left[f_m\left(\eta\right)-\chi_m f_{m-1}\left(\eta\right)\right]=\hbar_f\mathcal{R}_m^f\left(\eta\right), \tag{2.37}$$

$$f_m\left(0\right)=\frac{\alpha(1-n)}{1+n}f_m'(0), \tag{2.38}$$

$$f_m'(0)=1+\lambda f''(0),\quad f_m'\left(\infty\right)\rightarrow 0, \tag{2.39}$$

$$\mathcal{R}_m^f\left(\eta\right)=f_{m-1}'''+\sum_{k=0}^{m-1}\left(f_{m-1-k}f_k''-\frac{2n}{1+n}f_{m-1-k}'f_k'\right)$$

$$\chi_m=\begin{cases}0, & m\leq 1\\ 1, & m>1\end{cases}. \tag{2.40}$$

The general solution f_m having special function f_m^* is given by

$$f_m\left(\eta\right)=f_m^\star\left(\eta\right)+C_1+C_2e^{\eta}+C_3e^{-\eta}, \tag{2.41}$$

in which C_i, s for $i=1,2,3$ are the arbitrary constants.

2.4 HAM solution

Non-zero auxiliary parameter affects convergent series solution. Convergence region can be checked by drawing graphs of $\hbar_f$-curves for velocity distribution. Fig. 1 shows convergence region for velocity distribution keeping all other physical parameters constant. Admissible range for $\hbar_f$ is found $-1.7 \leq \hbar_f\ -0.2$.

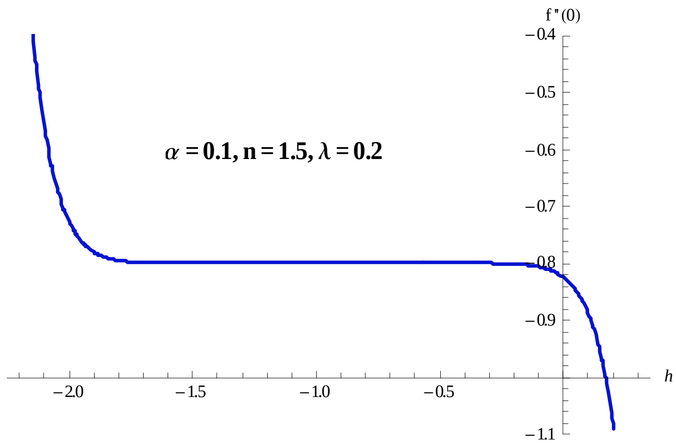

$\hbar$-curve for velocity

Tables 1 and 2 show comparison of different values of $-f''(0)$ in present work with those obtained by Fang et al. [19]

Table 1. Comparison of $-f''(0)$ in present work for $\alpha = 0.5$, $\lambda = 0$, with analysis of Fang et al. [19] :

n	10.0	9.0	7.0	5.0	3.0	2.0	1.0	0.50	0.00	-0.5
$-f''(0)$	1.0603	1.0589	1.0550	1.0486	1.0359	1.0234	1.0000	0.9799	0.9576	1.1667
present analysis	1.0603	1.0588	1.0551	1.0486	1.0358	1.0234	1.0000	0.9798	0.9577	1.1666

Table 2. Comparison of values of $-f''(0)$ in present work for $\alpha = 0.25$, $\lambda = 0$ with analysis of Fang et al. [19] :

n	10.0	9.0	7.0	5.0	3.0	1.0	1.0	0.0	$-1/3$	-0.5
$-f''(0)$	1.1433	1.1404	1.1323	1.1186	1.0905	1.0000	0.9338	0.78439	0.5000	0.0833
present analysis	1.1433	1.1404	1.1322	1.1186	1.0904	1.0000	0.9337	0.7843	0.5000	0.0832

2.5 Results and discussion

This section provides study of behaviors of pertinent parameters on velocity distribution. Both the above tables show a good agreement with previous existing literature. The results are illustrated graphically.

Behavior of slip velocity parameter on velocity distribution is shown in Fig. 2. Slip velocity parameter decreases the velocity distribution near surface of the sheet but it shows an increasing behavior at larger distances.

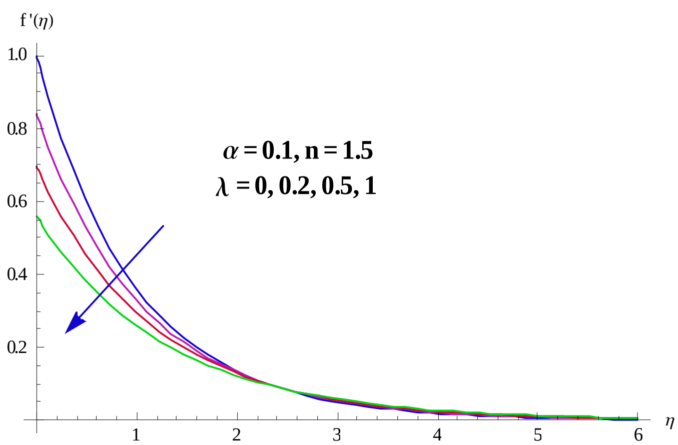

Fig. 2 Effect of λ on $f'(\eta)$.

Behavior of wall thickness parameter on velocity distribution is shown in Fig. 3. Two cases are shown for wall thickness parameter i.e. $n > 1$ and $n < 1$. Velocity profile shows a decreasing behavior for increasing values of wall thickness parameter when $n < 1$. Associated boundary layer thickness in this case also decreases.

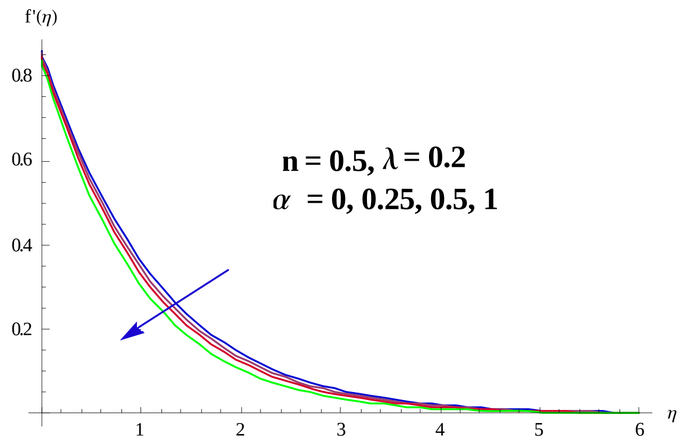

Fig. 3a Effect of α on $f'(\eta)$ for $n < 1$

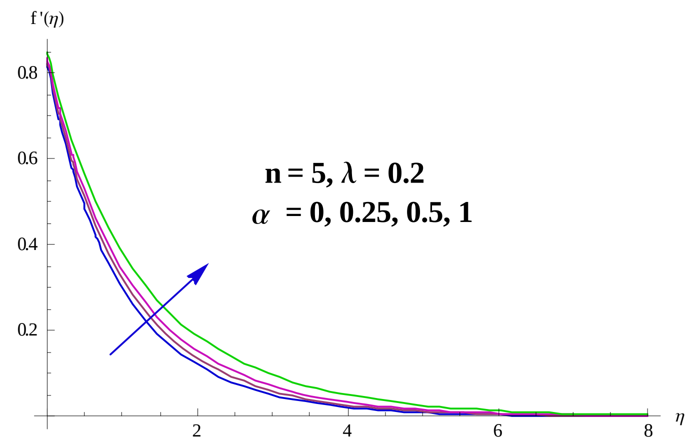

Fig. 3b Effect of α on $f'(\eta)$ for $n > 1$.

Fig.3b shows behavior of wall thickness on velocity for $n > 1$. It shows an increasing behavior from wall to the ambient fluid with increasing values of wall thickness when $n > 1$.

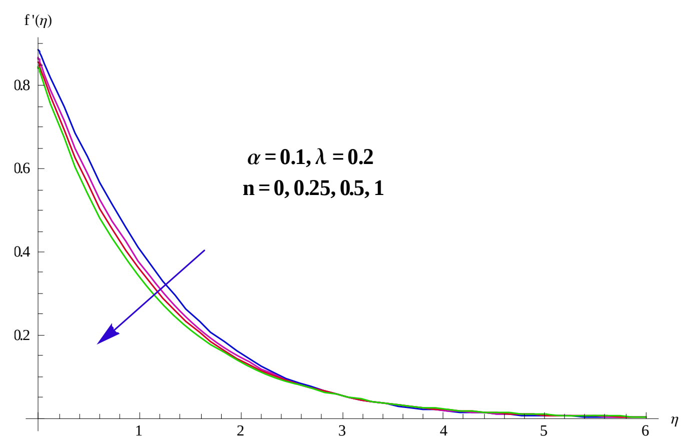

Fig. 4 Effect of n on $f'(\eta)$

Effect of velocity power index n on velocity profile is shown in Fig. 4. By increasing values of velocity power index, a decrease in velocity distribution occurs. Associated momentum layer thickness decays along the sheet for increasing n and a reverse process occurs away from the sheet. Table. 3 shows values of $-f''(0)$ for pertinent parameters.

Table. 3. Values for λ, α, and n

λ	α	n	$-f''(0)$
0.0	0.2	0.5	0.924828
0.2	0.2	0.5	0.728201
0.5	0.2	0.5	0.561082
0.2	0.0	0.5	0.707579
0.2	0.25	0.5	0.733395
0.2	0.5	0.5	0.759570
0.2	1.0	0.5	0.812747
0.2	0.0	5.0	0.890165
0.2	0.25	5.0	0.850600
0.2	0.5	5.0	0.812508
0.2	1.0	5.0	0.741247
0.2	0.2	0.0	0.611306
0.2	0.2	0.5	0.728201
0.2	0.2	2.0	0.819489
0.2	0.2	5.0	0.858401

Effects of pertinent parameters on skin friction are displayed in Table. 3. Table shows that velocity power index n and wall thickness parameter α enhance skin friction coefficient while slip velocity parameter decreases it. The slip condition leads to reduction of momentum transfer towards fluid. During slip condition the velocity of the sheet and fluid near the sheet is not same, i.e. less force is transferred to the fluid which results in reduction of velocity profile.

2.6 Main points

Flow characteristics of Newtonian fluid with variable thickness sheet and velocity slip are analyzed in this article. The present analysis was compared with previously existing literature and an excellent agreement is shown. Main points are as follows:

- Increase in velocity slip decreases skin friction coefficient.

- Skin friction is an increasing function of wall thickness parameter for $n < 1$ and it decreases for $n > 1$.
- Power index decreases velocity profile.

Chapter 3

Heat generation and Cattaneo-Christov heat flux effect in flow over a variable thicked stretching surface

3.1 Introduction

In this chapter the flow and heat transfer characteristics of an Oldroyd-B fluid over a non linearly stretching sheet with variable thickness are analyzed. Characteristics of heat transfer are investigated with temperature dependent thermal conductivity and heat source/sink. Cattaneo-Christov heat flux model is used rather than Fourier's law of heat conduction in present flow analysis. Thermal conductivity variation with temperature is considered. Resulting partial differential equations through conservation laws of mass, linear momentum and energy are converted into ordinary differential equations by suitable transformations. Convergent series solutions for velocity and temperature distribution are developed and discussed.

3.2 Development of problems

The steady and incompressible boundary layer flow of an Oldroyd-B fluid past a stretching sheet with variable thickness is analyzed here. We consider Cattaneo-Christov heat flux model instead of classical Fourier's law of heat conduction. Heat transfer is explored subject to temperature dependent thermal conductivity and heat generation/absorption. Cartesian coordinates are imposed such that x-axis is taken parallel to the sheet. Here y-axis is normal to x-axis. It is also assumed that wall temperature T_w is greater than ambient temperature T_∞ (i.e. $T_w > T_\infty$).

Governing equations for given problem are

$$\nabla.\mathbf{V} = \mathbf{0}, \tag{3.1}$$

and

$$\rho \frac{d\mathbf{V}}{d\bar{t}} = \operatorname{div}\mathbf{T} + \boldsymbol{\rho}\mathbf{B}. \tag{3.2}$$

We have no body forces so

$$\rho \frac{d\mathbf{V}}{d\bar{t}} = \operatorname{div}\mathbf{T}, \tag{3.3}$$

where $\mathbf{T}$ is Cauchy stress tensor given by

$$\mathbf{T} = -P\mathbf{I} + \mathbf{S}, \tag{3.4}$$

where μ is dynamic viscosity and $\mathbf{S}$ is extra stress tensor, given by

$$\mathbf{S} + \lambda_1 \frac{d\mathbf{S}}{dt} = \mu \left(1 + \lambda_2 \frac{D}{Dt}\right) \mathbf{A}_1, \tag{3.5}$$

here $\mathbf{A}_1$ is the first Rivelin Erickson tensor, λ_1 and λ_2 are relaxation and retardation times respectively.

For velocity

$$\mathbf{V} = \left(u(x,y), v(x,y), 0\right), \tag{3.6}$$

$$\mathbf{A}_1 = \operatorname{grad}\mathbf{V} + \left(\operatorname{grad}\mathbf{V}\right)^T. \tag{3.7}$$

Eq. $(3.1-3.7)$ for two dimensional flow yield

$$\frac{\partial u}{\partial x}+\frac{\partial v}{\partial y}=0, \tag{3.8}$$

$$\begin{aligned} & u\frac{\partial u}{\partial x}+v\frac{\partial u}{\partial y}+\lambda_1(u^2\frac{\partial^2 u}{\partial x^2}+2uv\frac{\partial^2 u}{\partial x\partial y}+v^2\frac{\partial^2 u}{\partial y^2}) \\ = & -\frac{1\partial p}{\rho\partial x}+\upsilon\left(\frac{\partial^2 u}{\partial x^2}+\frac{\partial^2 u}{\partial y^2}\right)+\upsilon\lambda_2\left(\begin{array}{c} u\left(\frac{\partial^3 u}{\partial x^3}+\frac{\partial^3 u}{\partial x\partial y^2}\right)+v\left(\frac{\partial^3 u}{\partial x^2\partial y}+\frac{\partial^3 u}{\partial y^3}\right) \\ -\left(\frac{\partial^2 u}{\partial x^2}+\frac{\partial^2 u}{\partial y^2}\right)\frac{\partial u}{\partial x}-\left(\frac{\partial^2 v}{\partial x^2}+\frac{\partial^2 v}{\partial y^2}\right)\frac{\partial u}{\partial y}\end{array}\right), \end{aligned} \tag{3.9}$$

and

$$u\frac{\partial v}{\partial x}+v\frac{\partial v}{\partial y}+\lambda_1(u^2\frac{\partial^2 v}{\partial x^2}+2uv\frac{\partial^2 v}{\partial x\partial y}+v^2\frac{\partial^2 v}{\partial y^2}) \tag{3.10}$$

$$= -\frac{1\partial p}{\rho\partial y}+\upsilon\left(\frac{\partial^2 v}{\partial x^2}+\frac{\partial^2 v}{\partial y^2}\right)+\upsilon\lambda_2\left(\begin{array}{c} u\left(\frac{\partial^3 v}{\partial x^3}+\frac{\partial^3 v}{\partial x\partial y^2}\right)+v\left(\frac{\partial^3 v}{\partial x^2\partial y}+\frac{\partial^3 v}{\partial y^3}\right) \\ -\left(\frac{\partial^2 u}{\partial x^2}+\frac{\partial^2 u}{\partial y^2}\right)\frac{\partial v}{\partial x}-\left(\frac{\partial^2 v}{\partial x^2}+\frac{\partial^2 v}{\partial y^2}\right)\frac{\partial v}{\partial y}\end{array}\right). \tag{3.11}$$

After applying the boundary layer approximations $(o(x)=o(u)=1, o(y)=o(v)=\delta)$ we have:

$$\frac{\partial u}{\partial x}+\frac{\partial v}{\partial y}=0, \tag{3.12}$$

$$\begin{aligned} & u\frac{\partial u}{\partial x}+v\frac{\partial u}{\partial y}+\lambda_1(u^2\frac{\partial^2 u}{\partial x^2}+2uv\frac{\partial^2 u}{\partial x\partial y}+v^2\frac{\partial^2 v}{\partial y^2}) \\ = & \upsilon\frac{\partial^2 u}{\partial y^2}+\lambda_2(u\frac{\partial^3 u}{\partial x\partial y^2}+v\frac{\partial^3 u}{\partial y^3}-\frac{\partial u\partial u^2}{\partial x\partial y^2}-\frac{\partial u\partial v}{\partial y\partial y^2}), \end{aligned} \tag{3.13}$$

$$\rho c_p\mathbf{v}\cdot\boldsymbol{\nabla}T=-\boldsymbol{\nabla}\cdot\mathbf{q}+Q(T-T_\infty). \tag{3.14}$$

Cattaneo-Christov heat flux model gives

$$\mathbf{q}+\tau_0\left(\frac{\partial\mathbf{q}}{\partial t}-\mathbf{q}\cdot\boldsymbol{\nabla}\mathbf{v}+\mathbf{v}\cdot\boldsymbol{\nabla}\mathbf{q}+(\boldsymbol{\nabla}\cdot\mathbf{v})\mathbf{q}\right)=-k(T)\boldsymbol{\nabla}T, \tag{3.15}$$

where τ_0 is relaxation time and $k(T)$ is temperature dependent thermal conductivity. It is noted that Eq. (3.14) reduces to classical Fourier's law when thermal relaxation parameter

$\tau_0 = 0$.

Fluid incompressibility declares that

$$\mathbf{q} + \tau_0 (\frac{\partial \mathbf{q}}{\partial t} + V \cdot \boldsymbol{\nabla} \mathbf{q} - \mathbf{q} \cdot \boldsymbol{\nabla} V) = -k(T) \boldsymbol{\nabla} T. \tag{3.16}$$

Equations (3.13) and (3.15) through elimination of $\mathbf{q}$ yields

$$\begin{aligned} & u\frac{\partial T}{\partial x} + v\frac{\partial T}{\partial y} + \tau_0 \left(u\frac{\partial u \partial T}{\partial x \partial x} + v\frac{\partial v \partial T}{\partial y \partial y} + u\frac{\partial v \partial T}{\partial x \partial y} + v\frac{\partial u \partial T}{\partial y \partial x} + 2uv\frac{\partial^2 T}{\partial x \partial y} + u^2\frac{\partial^2 T}{\partial x^2} + v^2\frac{\partial^2 T}{\partial y^2} \right) \\ = & \frac{Q}{\rho c_p}(T - T_\infty) + \tau_0 \frac{Q}{\rho c_p}(T - T_\infty) \left(u\frac{\partial T}{\partial x} + v\frac{\partial T}{\partial y} \right) + \frac{1}{\rho c_p}\frac{\partial}{\partial y}\left(k(T)\frac{\partial T}{\partial y} \right). \end{aligned} \tag{3.17}$$

The boundary conditions are

$$\begin{aligned} u &= U_w(x) = U_0 (x+b)^n, T = T_w \\ v &= 0, \text{ at } \quad y = A(x+b)^{\frac{1-n}{2}}, \end{aligned}$$

$$u \to 0, \quad T \to T_\infty, \text{ as } y \to \infty. \tag{3.18}$$

Here u and v denote the velocity components, U_w is stretching velocity, λ_1 is relaxation time, ν is kinematic viscosity of fluid, b is a dimensional constant, n is velocity power index, c_p is the specific heat, ρ is density, T is temperature, U_0 is the reference velocity, T_∞ is the ambient temperature of fluid, and variable thermal conductivity $k(T)$ is defined as:

$$k(T) = k_\infty (1 + \epsilon\theta), \tag{3.19}$$

where k_∞ is thermal conductivity of ambient fluid, θ is dimensionless temperature and ϵ is a small parameter showing the influence of temperature on thermal conductivity.

Utilizing the following transformations

$$
\begin{aligned}
\eta &= \sqrt{\frac{(n+1)U_0\,(x+b)^{n-1}}{2\nu}}y, \qquad \psi = \sqrt{\frac{2\nu U_0\,(x+b)^{n+1}}{n+1}}F\,(\eta)\,, \\
u &= U_0(x+b)F'\,(\eta)\,,\ v = -\sqrt{\frac{(n+1)\nu U_0\,(x+b)^{n-1}}{2}}\left(F(\eta)+\eta\frac{n-1}{n+1}F'(\eta)\right), \\
\theta\,(\eta) &= \frac{T-T_\infty}{T_w-T_\infty}, \qquad (3.20)
\end{aligned}
$$

the incompressibility condition is satisfied and Eqs. (3.12) and (3.16) become

$$F''' - \frac{2n}{n+1}F'^2 + FF'' + \beta 1\left(\begin{array}{c} (3n-1)FF'F'' - \frac{2n(n-1)}{n+1}F'^3 \\ -\frac{n+1}{2}F^2F''' + \eta\frac{n-1}{2}F''F'^2 \end{array}\right) \qquad (3.21)$$

$$+\beta 2\left(\frac{n-1}{2}F'F^3 + (\frac{3n-1}{2})F''^2 - \frac{n+1}{2}FF^{iv}\right) = 0, \qquad (3.22)$$

$$(1+\varepsilon\theta)\,\theta''+\varepsilon\theta'^2+\Pr F\theta'+\Pr\gamma(\frac{n-3}{2}FF'\theta'-\frac{n+1}{2}F^2\theta'')-\Pr\delta 1F\theta'+\frac{2}{n+1}\Pr\delta\theta=0, \quad (3.23)$$

The corresponding boundary conditions are

$$
\begin{aligned}
F'(\alpha) &= 1, \quad F\,(\alpha) = \frac{\alpha(1-n)}{1+n}, \quad F'\,(\infty)\to 0 \qquad (3.24) \\
\theta(\alpha) &= 1, \quad \theta\,(\infty)\to 0, \qquad (3.25)
\end{aligned}
$$

where $\delta 1$ is the heat generation/absorption in terms of thermal relaxation given by

$$\delta 1 = \frac{Q\tau_0}{\rho c_p} \qquad (3.26)$$

and δ is the heat generation/absorption given as:

$$\delta = \frac{Q}{\rho c_p U_0\,(x+b)^{n-1}}. \qquad (3.27)$$

The Prandtl number Pr is

$$\Pr = \frac{\mu c_p}{k_\infty} \qquad (3.28)$$

and

$$\alpha = \sqrt{\frac{n+1U_0}{2\nu}}. \tag{3.29}$$

Further by considering the transformation $F(\eta) = f(\eta - \alpha) = f(\xi)$, the non-dimensionalised governing equations are reduced along with the boundary conditions as follows:

$$f''' + ff'' - \frac{2n}{n+1}f'^2 + \beta 1 \begin{pmatrix} (3n-1)ff'f'' - \frac{2n(n-1)}{n+1}f'^3 \\ -\frac{n+1}{2}f^2f''' + \eta\frac{n-1}{2}f''f'^2 \end{pmatrix}$$

$$+\beta 1\left(\frac{n-1}{2}f'f^3 + (\frac{3n-1}{2})f''^2 - \frac{n+1}{2}ff^{iv}\right) = 0, \tag{3.30}$$

$$(1+\varepsilon\theta)\,\theta'' + \varepsilon\theta'^2 + \Pr f\theta' + \Pr\gamma\left(\frac{n-3}{2}ff'\theta' - \frac{n+1}{2}f^2\theta''\right) - \Pr\delta 1 f\theta' + \frac{2}{n+1}\Pr\delta\theta = 0, \tag{3.31}$$

$$\begin{aligned} f'(0) &= 1, \;\; f(0) = \frac{\alpha(1-n)}{1+n}, \;\; f'(\infty) \to 0, && (3.32) \\ \theta(0) &= 1, \;\; \theta(\infty) \to 0, && (3.33) \end{aligned}$$

3.3 Homotopic solutions

To develop the series solutions by HAM we select initial approximations and auxiliary linear operators. Initial guesses and linear operators here are

$$\begin{aligned} f_0(\eta) &= 1 - \exp(-\eta) + \alpha\frac{1-n}{1+n}, && (3.34) \\ \theta_0(\eta) &= \exp(-\eta), && (3.35) \end{aligned}$$

$$\mathcal{L}_f(f) = \frac{d^3 f}{d\eta^3} - \frac{df}{d\eta}, \qquad \mathcal{L}_\theta(\theta) = \frac{d^2\theta}{d\eta^2} - \theta, \tag{3.36}$$

with

$$\mathcal{L}_f\left[C_1 + C_2\exp(\eta) + C_3\exp(-\eta)\right] = 0, \tag{3.37}$$

$$\mathcal{L}_\theta\left[C_4\exp(\eta) + C_5\exp(-\eta)\right] = 0, \tag{3.38}$$

where C_i $(i = 1, 2, \ldots.., 5)$ denote the arbitrary constants.

3.3.1 Problems corresponding to zeroth-order

$$(1-p)\,\mathcal{L}_f\left[\widehat{f}\,(\eta;p)-f_0\,(\eta)\right]=p\hbar_f\mathcal{N}_f\left[\widehat{f}\,(\eta;p)\,,\widehat{\theta}\,(\eta;p)\right], \tag{3.39}$$

$$(1-p)\,\mathcal{L}_\theta\left[\widehat{\theta}\,(\eta;p)-\theta_0\,(\eta)\right]=p\hbar_\theta\mathcal{N}_\theta\left[\widehat{\theta}\,(\eta;p)\,,\widehat{f}\,(\eta;p)\right], \tag{3.40}$$

$$\widehat{f}\,(0;p)=\alpha\frac{1-n}{1+n},\quad \widehat{f}'\,(\infty;p)\to 0\quad \widehat{f}'\,(0;p)=1, \tag{3.41}$$

$$\widehat{\theta}\,(0;p)=0,\qquad \widehat{\theta}\,(\infty;p)\to 0, \tag{3.42}$$

$$\begin{aligned}\mathcal{N}_f\left[\widehat{f}\,(\eta,p)\,,\widehat{\theta}\,(\eta;p)\right]&=\frac{\partial^3\widehat{f}\,(\eta;p)}{\partial\eta^3}+\beta 1\left(\begin{array}{c}(3n-1)\,\widehat{f}\,(\eta;p)\,\frac{\partial\widehat{f}(\eta;p)}{\partial\eta}\frac{\partial^2\widehat{f}(\eta;p)}{\partial\eta^2}\\ -2n\left(\frac{n-1}{n+1}\right)\left(\frac{\partial\widehat{f}(\eta;p)}{\partial\eta}\right)^3+\eta(\frac{n-1}{2})\frac{\partial^2\widehat{f}(\eta;p)}{\partial\eta^2}(\frac{\partial\widehat{f}(\eta;p)}{\partial\eta})^2\\ -(\frac{n+1}{2})\widehat{f}\,(\eta;p)\,\frac{\partial^3\widehat{f}(\eta;p)}{\partial\eta^3}\end{array}\right)\\ &+\beta 2\left(\begin{array}{c}\frac{3n-1}{2}\left(\frac{\partial^2\widehat{f}(\eta;p)}{\partial\eta^2}\right)^2\\ +\left(\frac{n-1}{2}\right)\frac{\partial\widehat{f}(\eta;p)}{\partial\eta}\frac{\partial^2\widehat{f}(\eta;p)}{\partial\eta^2}\\ -\frac{n+1}{2}\widehat{f}\,(\eta;p)\,\frac{\partial^4\widehat{f}(\eta;p)}{\partial\eta^4}\end{array}\right)+\widehat{f}\,(\eta;p)\,\frac{\partial^2\widehat{f}\,(\eta;p)}{\partial\eta^2}-\frac{2n}{n+1}\left(\frac{\partial\widehat{f}\,(\eta;p)}{\partial\eta}\right)^2\end{aligned} \tag{3.43}$$

$$\begin{aligned}\mathcal{N}_\theta\left[\widehat{\theta}\,(\eta;p)\,,\widehat{f}\,(\eta;p)\right]&=\left(1+\varepsilon\widehat{\theta}\,(\eta;p)\right)\frac{\partial^2\widehat{\theta}(\eta,p)}{\partial\eta^2}\\ &+\Pr\widehat{f}\,(\eta;p)\,\frac{\partial\widehat{\theta}(\eta,p)}{\partial\eta}+\varepsilon\left(\frac{\partial\widehat{\theta}(\eta,p)}{\partial\eta}\right)^2\\ &+\Pr\gamma\left(\begin{array}{c}\frac{n-3}{2}\widehat{f}\,(\eta;p)\,\frac{\partial\widehat{f}(\eta;p)}{\partial\eta}\frac{\partial\widehat{\theta}(\eta,p)}{\partial\eta}\\ -\frac{n+1}{2}\left(\widehat{f}\,(\eta;p)\right)^2\frac{\partial^2\widehat{\theta}(\eta,p)}{\partial\eta^2}+\end{array}\right)\\ &-\Pr\delta 1\left(\widehat{f}\,(\eta;p)\,\frac{\partial\widehat{\theta}\,(\eta;p)}{\partial\eta}\right)+\frac{2}{n+1}\Pr\delta\widehat{\theta}\,(\eta;p)\,,\end{aligned} \tag{3.44}$$

in which $p\in[0,1]$ is the embedding parameter and $\hbar_f$, $\hbar_\theta$ the non-zero auxiliary parameters.

3.3.2 Problems corresponding to mth-order

$$\mathcal{L}_f\left[f_m\,(\eta)-\chi_m f_{m-1}\,(\eta)\right]=\hbar_f\mathcal{R}^f_m\,(\eta)\,, \tag{3.45}$$

$$\mathcal{L}_\theta\left[\theta_m\,(\eta)-\chi_m\theta_{m-1}\,(\eta)\right]=\hbar_\theta\mathcal{R}^\theta_m\,(\eta)\,, \tag{3.46}$$

$$f_m\,(0)=0,\quad f'_m\,(0)=0,\ \ f'_m\,(\infty)=0, \tag{3.47}$$

$$\theta_m(0) = 0, \quad \theta_m(\infty) = 0, \tag{3.48}$$

$$\begin{aligned}
\mathcal{R}_m^f(\eta) &= f'''_{m-1} + \sum_{k=0}^{m-1}\left(f_{m-1-k}f''_k - \frac{2n}{1+n}f'_{m-1-k}f'_k\right) \\
&+\beta 1\left(\begin{array}{c} \sum_{k=0}^{m-1} f_{m-1-k}\sum_{l=0}^{k}\left((3n-1)f'_{k-l}f''_l - \frac{n+1}{2}f_{k-l}f'''_l)\right) \\ +\sum_{k=0}^{m-1} f'_{m-1-k}\sum_{l=0}^{k}(\eta(\frac{n-1}{2})f'_{k-l}f''_l - \frac{2n(n-1)}{n+1}f'_{k-l}f'_l) \end{array}\right) \\
&+\beta 2\left(\sum_{k=0}^{m-1}(\frac{3n-1}{2}f''_{m-1-k}f''_k + (n-1)f'_{m-1-k}f'''_k - \frac{n+1}{2}f_{m-1-k}f^{iv}_k)\right)
\end{aligned} \tag{3.49}$$

$$\begin{aligned}
\mathcal{R}_m^\theta(\eta) &= \theta''_{m-1} + \varepsilon\sum_{k=0}^{m-1}\left(\theta_{m-1-k}\theta''_k\right) + \varepsilon\sum_{k=0}^{m-1}\theta''_{m-1-k}\theta''_k \\
&+ \Pr\gamma\sum_{k=0}^{m-1} f_{m-1-k}\sum_{l=0}^{k}\left(f'_{k-l}\theta_l - \frac{n+1}{2}f_{k-l}\theta''_l\right) \\
&- \Pr\delta 1\sum_{k=0}^{m-1} f_{m-1-k}\theta'_k + \frac{2}{n+1}\Pr\delta\theta_{m-1},
\end{aligned} \tag{3.50}$$

$$\chi_m = \begin{cases} 0, & m \le 1 \\ 1, & m > 1 \end{cases}. \tag{3.51}$$

For $p = 0$ and $p = 1$, we can write

$$\widehat{f}(\eta; 0) = f_0(\eta), \quad \widehat{f}(\eta; 1) = f(\eta), \tag{3.52}$$

$$\widehat{\theta}(\eta; 0) = \theta_0(\eta), \quad \widehat{\theta}(\eta; 1) = \theta(\eta), \tag{3.53}$$

and when p varies from 0 to 1, $\widehat{f}(\eta; p)$ and $\widehat{\theta}(\eta; p)$ vary from initial solutions $f_0(\eta)$ and $\theta_0(\eta)$ to final solutions $f(\eta)$ and $\theta(\eta)$ respectively. Through Taylor series expansion we have

$$\widehat{f}(\eta; p) = f_0(\eta) + \sum_{m=1}^{\infty} f_m(\eta)p^m, \quad f_m(\eta) = \frac{1}{m!}\frac{\partial^m \widehat{f}(\eta; p)}{\partial p^m}\bigg|_{p=0}, \tag{3.54}$$

$$\widehat{\theta}(\eta; p) = \theta_0(\eta) + \sum_{m=1}^{\infty} \theta_m(\eta)p^m, \quad \theta_m(\eta) = \frac{1}{m!}\frac{\partial^m \widehat{\theta}(\eta; p)}{\partial p^m}\bigg|_{p=0}. \tag{3.55}$$

The value of auxiliary parameter is chosen such that the series (3.54) and (3.55) converge at $p = 1$ i.e.

$$f(\eta) = f_0(\eta) + \sum_{m=1}^{\infty} f_m(\eta), \tag{3.56}$$

$$\theta(\eta) = \theta_0(\eta) + \sum_{m=1}^{\infty} \theta_m(\eta). \tag{3.57}$$

Denoting general solutions (f_m, θ_m) of Eqs. (3.45) and (3.46) and special solutions (f_m^*, θ_m^*) we have

$$f_m(\eta) = f_m^{\star}(\eta) + C_1 + C_2 e^{\eta} + C_3 e^{-\eta}, \tag{3.58}$$

$$\theta_m(\eta) = \theta_m^{\star}(\eta) + C_4 e^{\eta} + C_5 e^{-\eta}, \tag{3.59}$$

where the constants C_i $(i = 1 - 5)$ through the boundary conditions (3.37) and (3.38) are

$$\begin{aligned} C_2 &= C_4 = 0, \qquad C_3 = \left.\frac{\partial f_m^{\star}(\eta)}{\partial \eta}\right|_{\eta=0}, \\ C_1 &= -C_3 - f_m^{\star}(0), \quad C_5 = -\theta_m^{*}(0). \end{aligned} \tag{3.60}$$

3.4 Convergence analysis

To show convergence of obtained series solutions, it is necessary to display the $\hbar$-curves. The region of the graph parallel to the $\hbar$-axis represents the interval of convergence. Hence $\hbar$-curves are plotted in Figs. 1 and 2. The admissible ranges of $\hbar_f$ and $\hbar_\theta$ are noted $-1.1 \leq \hbar_f \leq -0.3$ and $-2 \leq \hbar_\theta \leq -0.3$ and for f and θ respectively.

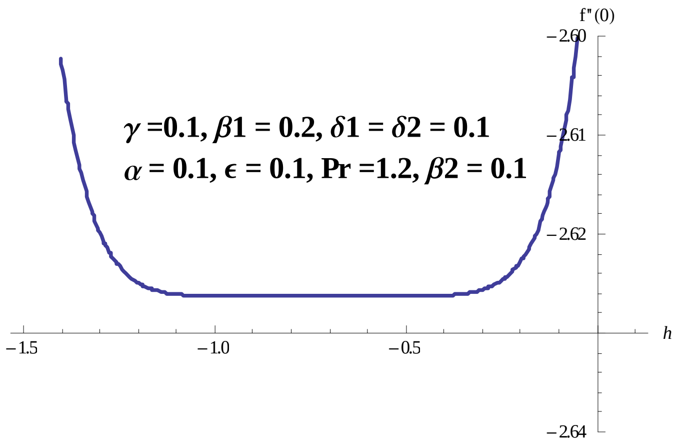

Fig. 1. $\hbar$-curve for $f'(\eta)$

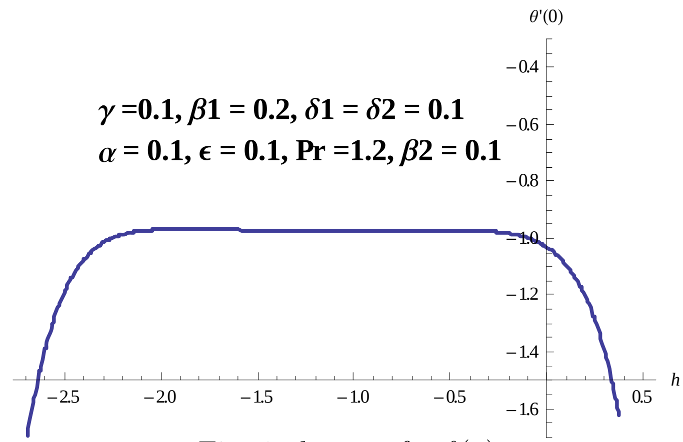

Fig. 2. $\hbar$-curve for $\theta(\eta)$

3.5 Discussion

This subsection has been prepared for the discussion of velocity and temperature. Fig. 3 depicts the velocity for the influence of Deborah number $\beta 1$ (in terms of relaxation time). It is observed that higher Deborah number results in the reduction of velocity profile. Since Deborah number shows the ratio of relaxation to observation time. Thus more resistance is noticed to the fluid motion when Deborah number enhances and so velocity decays. Effect of wall thickness parameter on velocity distribution is shown in Fig. 4. Velocity distribution has a decreasing influence for increasing values of wall thickness parameter. Behavior of Deborah number (in terms of retardation time) $\beta 2$ on velocity is shown in Fig. 5. Velocity profile shows an increasing effect of $\beta 2$, and associated velocity boundary layer thickness. Impact of ϵ on temperature distribution is shown in Fig. 6. Higher values of ϵ results in enhancement of temperature profile. In fact higher values of ϵ corresponds to large thermal conductivity which gives an increase in temperature profile. Fig. 7 represents the effect of thermal relaxation parameter γ on temperature profile. Thermal relaxation time is a commonly used parameter for estimating the time required of heat to conduct or transfer to any other material or any part of the same material. It is analyzed that temperature distribution shows a decreasing behavior for higher thermal relaxation parameter. By increasing γ, the particles of material need extra time to conduct heat to its neighboring particles. Or we can say that by increasing the values of γ, the material shows a non-conducting behavior which results in decrease of temperature distribution. Influence of heat generation parameter δ is sketched in Fig. 8. Higher values of heat generation parameter yield to an enhancement of temperature distribution and associated thermal boundary layer thickness. It is due to the fact that more heat is produced during the heat generation process and ultimate temperature distribution enhances. Behavior of Prandtl number on temperature distribution is shown in Fig. 9. Temperature is noted as decreasing function of Pr. Physically Pr is the ratio of momentum to thermal diffusivities. For larger values of Prandtl number, the thermal diffusivity decreases which is the reason for the decrease in temperature distribution. Behavior of temperature distribution due to the heat generation/absorption parameter in terms of thermal relaxation $\delta 1$ is shown in Fig. 10. It is concluded that temperature distribution increases for larger values of heat generation parameter in terms of thermal relaxation. Also thermal boundary layer thickness enhances.

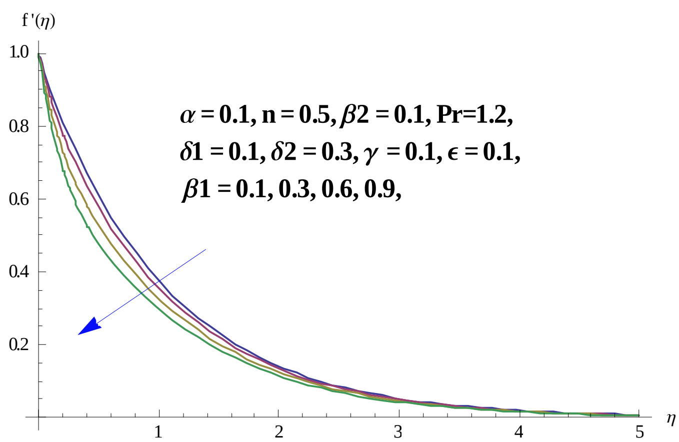

Fig. 3 Plot of on f' for $\beta 1$.

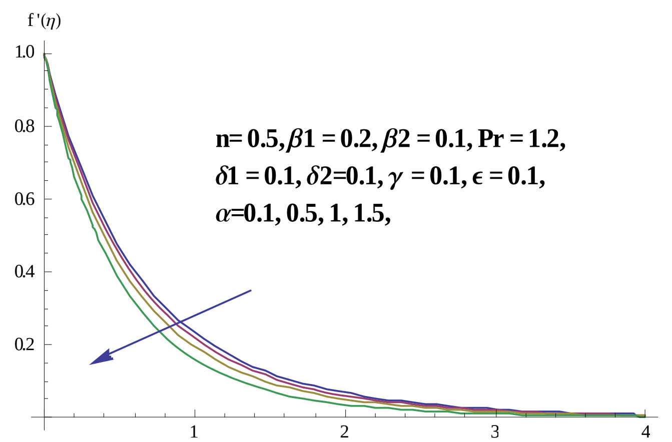

Fig. 3 Plot of on f' for $\beta 1$.

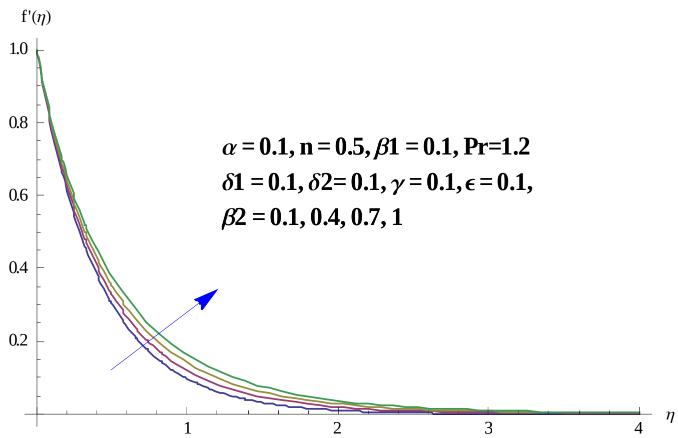

Fig. 5 Plot of on f' for $\beta 2$.

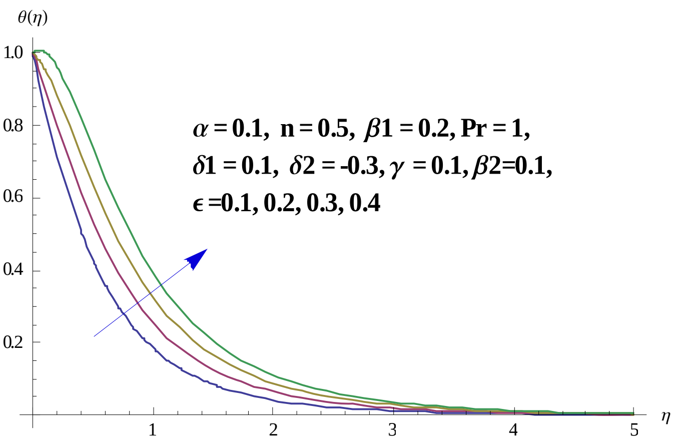

Fig. 6 Plot of on θ for ϵ.

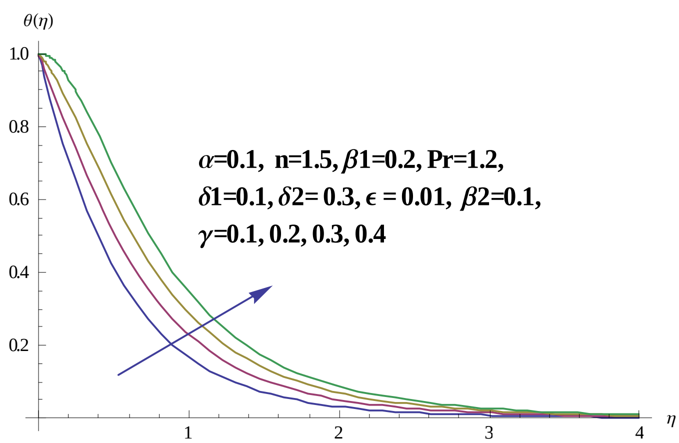

Fig. 7. Plot of θ for γ.

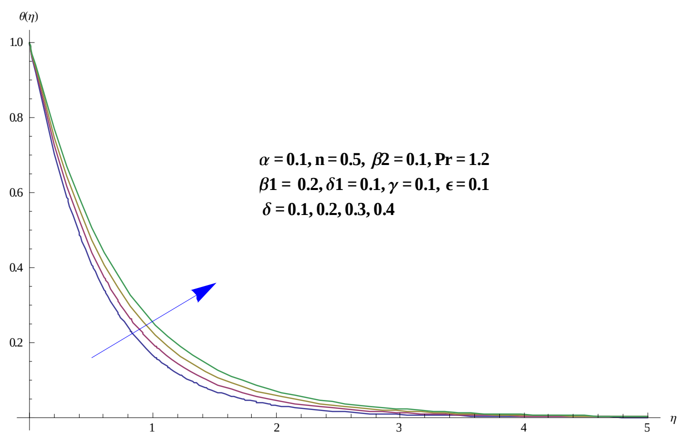

Fig. 8. Plot of θ for δ.

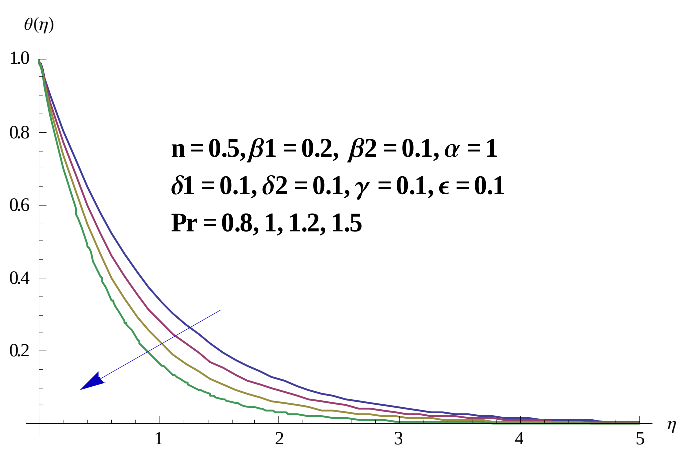

Fig. 9. Plot of θ for Pr.

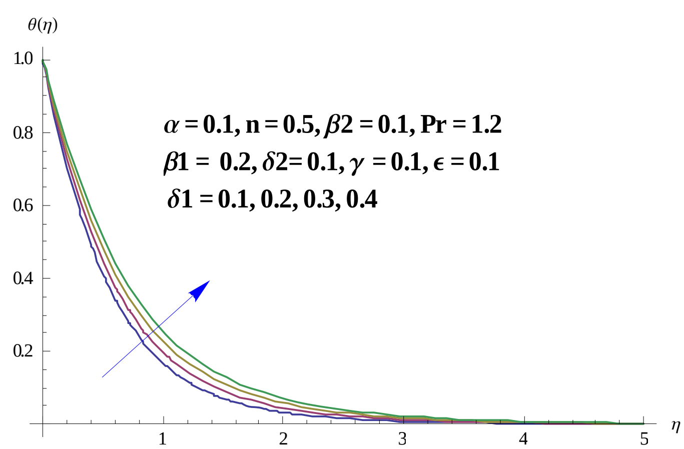

Fig. 10. Plot of θ for $\delta 1$.

3.6 Conclusions

Flow of an Oldroyd-B fluid in presence of Cattaneo-Christov theory and variable surface thickness is studied. We at present have outcomes as follows:

- Both velocity and layer thickness decrease for larger Deborah number corresponding to relaxation time.
- Higher values of wall thickness parameter decrease the velocity distribution.
- Thermal relaxation parameter results in the reduction of temperature distribution.
- Higher temperature is observed for larger values of ϵ.
- Heat generation in terms of thermal relaxation enhances temperature distribution and associated thermal boundary layer thickness.

Bibliography

[1] J. B. J. Fourier, Theorie analytique De Lachaleur, Paris, 1822.

[2] C. Cattaneo, Sulla conduzione del calore, Atti Semin. Mat. Fis. Univ. Modena ReggioEmilia 3 (1948) 83-101.

[3] C. I. Christov, On frame indifferent formulation of the Maxwell-Cattaneo model of finite speed heat conduction. Mech. Res. Commun. 36 (2009) 481-486.

[4] B. Straughan, Thermal convection with the Cattaneo-Christov model. Int. J. Heat Mass Transfer 53 (2010) 95-98.

[5] V. Tibullo and V. Zampoli, A uniqueness result for the Cattaneo-Christov heat conduction model applied to incompressible fluids. Mech. Res. Commun. 38 (2011) 77-99.

[6] S. Han, L. Zheng, C. Li and X. Zhang, Coupled flow and heat transfer in viscoelastic fluid with Cattaneo-Christov heat flux model. Appl. Math. Lett. 38 (2014) 87-93.

[7] M. Mustafa, Cattaneo-Christov heat flux model for rotating flow and heat transfer of upper convected Maxwell fluid. AIP Advances 5 (2015) 047109.

[8] T. Hayat, M. Farooq, A. Alsaedi and Falleh Al-Solamy, Impact of Cattaneo-Christov heat flux in the flow over a stretching sheet with variable thickness. AIP Advances 5 (2015) 087159.

[9] L. Zheng, L. Wang and X. Zhang, Analytic solutions of unsteady boundary layer flow and heat transfer on a permeable stretching sheet with non-uniform heat source/sink. Commun. Nonlinear Sci. Numer. Simulat. 16 (2011) 731-740.

[10] M. M. Rashidi, N. V. Ganesh, A. K. A. Hakeem and B. Ganga, Buoyancy effect on MHD flow of nanofluid over a stretching sheet in the presence of thermal radiation. J. Mol. Liq.198 (2014) 234-238.

[11] X. Su, L. Zheng, X. Zhang and J. Zhang, MHD mixed convective heat transfer over a permeable stretching wedge with thermal radiation and Ohmic heating. Chem. Eng. Sci. 78 (2012) 1-8.

[12] M. Turkyilmazoglu, Three dimensional MHD flow and heat transfer over a stretching/shrinking surface in a viscoelastic fluid with various physical effects. Int. J. Heat Mass Transfer 78 (2014) 150-155.

[13] L. Zheng, J. Niu, X. Zhang and Y. Gao, MHD flow and heat transfer over a porous shrinking surface with velocity slip and temperature jump. Math. Comptuer Model. 56 (2012) 133-144.

[14] T. Hayat, S. Asad, M. Mustafa and A. Alsaedi, MHD stagnation point flow of Jeffrey fluid over a convectively heated stretching sheet. Computers & Fluids 108 (2015) 179-185.

[15] L. Zheng, N. Liu and X. Zhang, Maxwell fluids unsteady mixed flow and radiation heat transfer over a stretching permeable plate with boundary slip and non-uniform heat source/sink. ASME. J. Heat Transfer 135 (2013) 031705.

[16] S. Mukhopadhyay, K. Bhattacharyya and G. C. Layek, Mass transfer over an exponentially stretching porous sheet embedded in a stratified medium. Chem. Eng. Commun. 201 (2014) 272-286.

[17] T. Hayat, Z. Hussain, M. Farooq, A. Alsaedi and M. Obaid, Thermally stratified stagnation point flow of an Oldroyd-B fluid. Int. J. Nonlinear Sci. Numer. Simul. 15 (2014) 77-86.

[18] M. Sheikholeslami and D. D. Ganji, Numerical investigation for two phase modeling of nanofluid in a rotating system with permeable sheet. J. Mol. Liq. 194 (2014) 13-19.

[19] T. Fang, J. Zhang and Y. Zhong, Boundary layer flow over a stretching sheet with variable thickness. Appl. Math. Comput. 218 (2012) 7241-7252.

[20] M. M. Khader and A. M. Megahed, Numerical solution for boundary layer flow due to a nonlinearly stretching sheet with variable thickness and slip velocity. Eur. Phys. J. Plus 128 (2013) 100.

[21] M. S. A. Wahed, E. M. A. Elbashbeshy and T. G. Emam, Flow and heat transfer over a moving surface with non-linear velocity and variable thickness in a nanofluids in the presence of Brownian motion. Appl. Math. Comput. 254 (2015) 49-62.

[22] S. J. Liao, Homotopy analysis method in non-linear differential equations, Springer and Higher Education Press, Heidelberg (2012).

[23] S. Abbasbandy, M. S. Hashemi and I. Hashim, On convergence of homotopy analysis method and its application to fractional integro-differential equations. Quaestiones Mathematicae 36 (2013) 93—105.

[24] T. Hayat, M. Farooq and A. Alsaedi, Thermally stratified stagnation point flow of Casson fluid with slip conditions. Int. J. Numer. Methods Heat Fluid Flow 25 (2015) 724-748.

[25] M. Turkyilmazoglu, Solution of the Thomas-Fermi equation with a convergent approach. Commun. Nonlinear Sci. Numer. Simulat. 17, (2012) 4097-4103.

[26] S. A. Shehzad, T. Hayat, M. S. Alhuthali and S. Asghar, MHD three-dimensional flow of Jeffrey fluid with Newtonian heating. J. Central South Univ. 21 (2014) 1428-1433.

[27] O. Abu Arqub and A. El-Ajou, Solution of the fractional epidemic model by homotopy analysis method. J.King Saud University Science 25 (2013) 73-81.

[28] T. Hayat, A. Shafiq, M. Imtiaz and A. Alsaedi, Impact of melting phenomenon in the Faulkner-Skan Wedge flow of second grade nanofluid: A revised model. J. Mol. Liquids 215 (2016) 664-670.

[29] T. Hayat, M. Imtiaz and A. Alsaedi, Unstedy flow of nanofluid with double stratification and magnetohydrodynamics. Int. J. Heat Mass Transfer. 92 (2016) 100-109.